Saturated absorption spectroscopy near 1.57 μm and revised rotational line list of $^{12}C^{16}O$

J. Wang [a,b], C.-L. Hu [a,b], A.-W. Liu [a,b,*], Y.R. Sun [a,b], Y. Tan [a,b], S.-M. Hu [a,b]

[a] Hefei National Laboratory for Physical Sciences at Microscale, iChem Center, University of Science and Technology of China, Hefei 230026, China
[b] CAS Center for Excellence and Synergetic Innovation Center in Quantum Information and Quantum Physics, University of Science and Technology of China, Hefei 230026, China

ARTICLE INFO

ABSTRACT

Molecular transitions provide natural frequency standards for spectroscopy, telecommunication, and astrophysics. The frequency accuracy is also crucial in various tests of fundamental physics. A comb-locked cavity ring-down spectrometer measured lamb dips of sixty-one $^{12}C^{16}O$ transitions around 1.57 μm in the second overtone band. The positions were determined with an accuracy of a few kHz. A new set of rotational spectroscopic parameters was derived with 30 ground state combination difference for the ground vibrational state with a standard deviation of 4.5 kHz. It results in a refinement of the ro-vibrational spectroscopic constants for the $v=3$ vibrational state. These parameters allow the pure rotational line lists of the $v = 0 \leftarrow 0$ and $v = 3 \leftarrow 3$ in the 112 GHz – 3.89 THz regions.

1. Introduction

As the most stable and second abundant diatomic molecule, carbon monoxide (CO) has been extensively studied both in the laboratory and astrophysics. Numerous spectroscopic parameters of CO have been gathered from microwave to the ultraviolet regions. They are essential for CO observations in the planets [1] and exoplanets [2] from space and the ground.

Its pure rotational transitions are present in local luminous infrared galaxies (LIRGs) [3], asymptotic giant branch (AGB) stars [4], and other interstellar mediums [5], aid in the understanding the C/O abundance, the molecular gas kinetic temperature, and the planetary atmospheric properties. The high-resolution spectroscopy in the near-infrared region has been used to explore terrestrial mass planets around M dwarfs [6] and the long-awaited Sun-Earth analog system [7]. This method is sensitive mainly to the line positions [2].

On the other side, more and more precise line frequencies will also satisfy the growing need for convenient wavelength standards for the wavelength-division multiplexing systems in optical communications. For example, Bureau International des Poids et Mesures recommended the C_2H_2 line positions near 1.54 μm as the secondary frequency standards for length metrology. In recent years, considerable efforts [8–12] have been carried out to enable the possibility of the saturated absorption spectroscopy of weak molecular transition with a frequency accuracy of a few kHz in the near-infrared region. It will lead to more and more frequency standards and be beneficial for the retrieval of high accurate line profile parameters.

Recently, we have developed a comb-locked cavity ring-down spectrometer that enables the saturated absorption spectroscopy of molecular transitions in the near-infrared region with a frequency accuracy of a few kHz and a sensitivity of 10^{-12} cm^{-1} [12,13]. Here we report the Doppler-free saturation spectroscopy of $^{12}C^{16}O$ ro-vibrational transitions in the second overtone band near 1.57 μm for P(31)- R(29) 61 lines. The absolute transition frequencies were determined to a few kHz for these lines covering a wide intensity range by three orders of magnitude. After describing the experimental setup in Section 2, we will detail the frequency and uncertainty analysis and comparisons to previously available data in the literature in Section 3.

2. Experimental details

The experiment setup consists of frequency locking and spectral probing, similar to our recently developed comb-locked cavity ring-down saturation spectrometers described in detail in refs. [12–18]. A tunable external-cavity diode laser (ECDL, Toptica DLC Pro-1550) is split into two beams by a polarizing beam splitter. The s-polarization laser beam is locked to a temperature-stabilized ring-down cavity using the Pound-Drever-Hall (PDH) method. The cavity length is stabilized through a piezo actuator (PZT) driven by

---

* Corresponding author.
  E-mail address: awliu@ustc.edu.cn (A.-W. Liu).

a phase-lock circuit based on the beat signal between the probe laser and an optical frequency comb. The frequency comb is synthesized by an Er: fiber oscillator operated at 1.56 um. The repetition rate ($f_r \approx 184$MHz) and carrier off frequency ($f_0 = 20$MHz) are both locked to a Radio-Frequency source which is referenced to a Global Positioning System (GPS) disciplined rubidium clock (SpectraTime GPS Reference 2000). The p-polarization beam passes an acousto-optic modulator (AOM) and a fiber electro-optic modulator (EOM). A single selected sideband of EOM is then coupled into the cavity to produce the ring-down signal, separated from the locking beam with a combination of polarizing waveplates and Glan-Taylor prisms. The laser power used for spectral probing was between 1.5 and 14 mw, resulting in the intra-cavity laser powers of 7~110 W for 61 measured transitions at respective pressures [12,19].

The AOM also serves as a beam chopper, triggered by an external rectangle wave to block the probing beam to initial a ring-down event. An exponential decay function fits the ring-down curve to derive the decay time τ. The sample absorption coefficient α is determined from the change of the cavity loss rate: $\alpha = (c\tau)^{-1} - (c\tau_0)^{-1}$, where c is the speed of light, and τ_0 is the decay time of the empty cavity. The saturated absorption spectra are measured by tuning the reference frequency f_B of the phase-lock loop: $\nu = f_0 + N \times f_{rep} + f_B + f_{AOM} + f_{EOM}$, where f_{AOM} and f_{EOM} are the radio frequency driving the AOM and EOM.

Two cavities with different lengths and mirrors were used in this experiment to achieve the saturated absorption spectrum of the second overtone band of $^{12}C^{16}O$ in the spectral range of 1562 - 1619 nm. The two cavities' length is 44.6 cm and 108 cm, related to about 336 MHz and 138 MHz of the free spectral ranges (FSR), respectively. The mirrors' reflectivity is about 99.998% and 99.997% at 1.5 – 1.7 μm (Layertec GmbH). Therefore, the RD cavities have the fineness of about 1.5×10^5 and 1.36×10^5, and the mode width is about 2.2 kHz and 1 kHz.

The measurements were performed at room temperature(298 ± 0.1K). The saturated absorption spectrum of the relatively stronger transitions with J$\leq$19 was measured with the shorter cavity. The longer cavity with better signal-to-noise was used to measure the transitions with J$>$19. Gas sample was bought from Nanjing Special Gas Co. with a stated purity of 99.99% and purified with a "freeze-pump-thaw" process before measurement. The gas pressures in the range of 0.3 – 2.4 Pa were adopted in this work.

3. Results and discussions

3.1. Absolute frequencies of 61 lines

Fig. 1 shows the averaged spectra of the R(7) and P(31) lines over a span of 4 MHz. The line parameters, including the Lamb-dip center, the width, and the Lamb-dip depth, were derived from the saturated absorption spectrum fit with a Lorentzian function. Residuals are illustrated in the lower panels of Fig. 1 for strong (10^{-23} cm • molecule^{-1}) and weak (10^{-26} cm • molecule^{-1}) transitions recorded with the sample pressures of 0.3 and 2.4 Pa, respectively. The retrieved linewidth of R(7) and P(31) are about 350 kHz and 700 kHz, which are close to the values of the saturated absorption of $^{12}C^{16}O_2$ recorded with similar pressures [18]. The noise level reaches about 1×10^{-12} cm^{-1}, with the spectrum averaged from 200 scans recorded in 6 hours. The dip depths of 61 lines vary from 2×10^{-11} to 9×10^{-9} cm^{-1} depending on the line intensities in the range of 8.60×10^{-27} – 2.16×10^{-23} cm • molecule^{-1}. It leads to 60 ~ 1000 signal-to-noise levels for the transitions measured in this work.

The uncertainty of the line frequency is composed of statistic and systematic uncertainties. The former mostly depends on the signal-to-noise and the linewidth, which are less than 12 kHz for all 61 lines. The systematic uncertainty sources include (i) fre-

quency comb, (ii) AOM and EOM, (iii) cavity locking servo, (iv) power shift, (v) pressure shift, (vi) line profile asymmetry, (vii) the second-order Doppler shift.

(i) The long-term stability of 2×10^{-12} from the GPS-disciplined rubidium clock introduces an uncertainty of 0.4 kHz around 1.57 μm to the laser frequency calibration with the frequency comb.

(ii) The uncertainties in the driving frequencies of the AOM and EOM are negligible [12,13].

(iii) The Allan deviation of the beat frequency between the probe laser and the frequency comb allows the estimated uncertainty of about 0.4 kHz due to the bias in the cavity locking servo.

(iv) No difference is found in the line position within the experimental uncertainty using a different input laser power in the measurement.

(v) Similar to that discussed in our previous studies of C_2H_2 [17], HD [16], and CO_2 [18], no significant pressure shifts are observed for the line positions measured within 2.5 Pa. Therefore, an uncertainty of 0.2 kHz is given for a possible contribution from the pressure-induced coefficient determined in ref. [13].

(vi) The uncertainty in the range of 0.2 – 25 kHz is assigned for the possible asymmetry due to the line profile model, although no asymmetry is observed above the noise level.

(vii) Taking a root-square mean velocity of 515 m/s of the $^{12}C^{16}O$ molecule at 298 K, the second-order Doppler shift is 0.28 kHz with a negligible uncertainty.

The positions of 61 lines in the second overtone band of $^{12}C^{16}O$ are summarized in Table I, together with the uncertainties.

3.2. Spectroscopic analysis of ro-vibrational transition frequencies

The ro-vibrational energy of $^{12}C^{16}O$ molecule can be expressed with a simple model:

$$E(J) = G_\upsilon + B_\upsilon J(J+1) - D_\upsilon J^2(J+1)^2 + H_\upsilon J^3(J+1)^3 \\ + L_\upsilon J^4(J+1)^4 + \cdots \quad (1)$$

where G_v is the vibrational term, B_v is the rotational constants, D_v, H_v, and L_v are centrifugal distortion constants, J corresponds to the angular momentum quantum number.

Then the line positions can be analyzed with two sets of the ground state constants were determined with the CDMS (Cologne) values [20] and NIST values [21]. However, most ro-vibrational energy levels of υ=3 state cannot be reproduced very well by these two sets of spectroscopic constants. The line position difference between the calculated and experimental values is over 3-σ experimental uncertainties for 23 and 33 transitions with NIST and Cologne's constants.

As the ground state parameters retrieved with the ro-vibrational spectroscopy for some symmetric molecules $^{12}C_2H_2$ [22], $^{13}C_2H_2$ [23,24], and $^{12}C^{16}O_2$ [18], the ground state spectroscopic constants of $^{12}C^{16}O$ can also be independently retrieved by fitting 30 ground state combination difference determined from this work with the formula given below:

$$\Delta_2 F'' = \nu_{R(J-1)} - \nu_{P(J+1)} = \left(4B'' - 6D'' + \frac{27}{4}H'' + \frac{27}{4}L''\right)\left(J + \frac{1}{2}\right) \\ + (-8D'' + 34H'' + 75L'')(J + \frac{1}{2})^3 \quad (2) \\ + (12H'' + 100L'')(J + \frac{1}{2})^5 + 16L''(J + \frac{1}{2})^7 + \cdots$$

where $\nu_{R(J-1)}$ and $\nu_{P(J+1)}$ are the frequencies of the lines R(J-1) and P(J+1), respectively. The second overtone excited state spectroscopic constants except the vibrational term G_υ can be similarly fitted to:

$$\Delta_2 F'' = \nu_{R(J)} - \nu_{P(J)} = \left(4B' - 6D' + \frac{27}{4}H' + \frac{27}{4}L'\right) \\ \left(J + \frac{1}{2}\right) + (-8D' + 34H' + 75L')(J + \frac{1}{2})^3 \quad (3) \\ + (12H' + 100L')(J + \frac{1}{2})^5 + 16L'(J + \frac{1}{2})^7 + \cdots$$
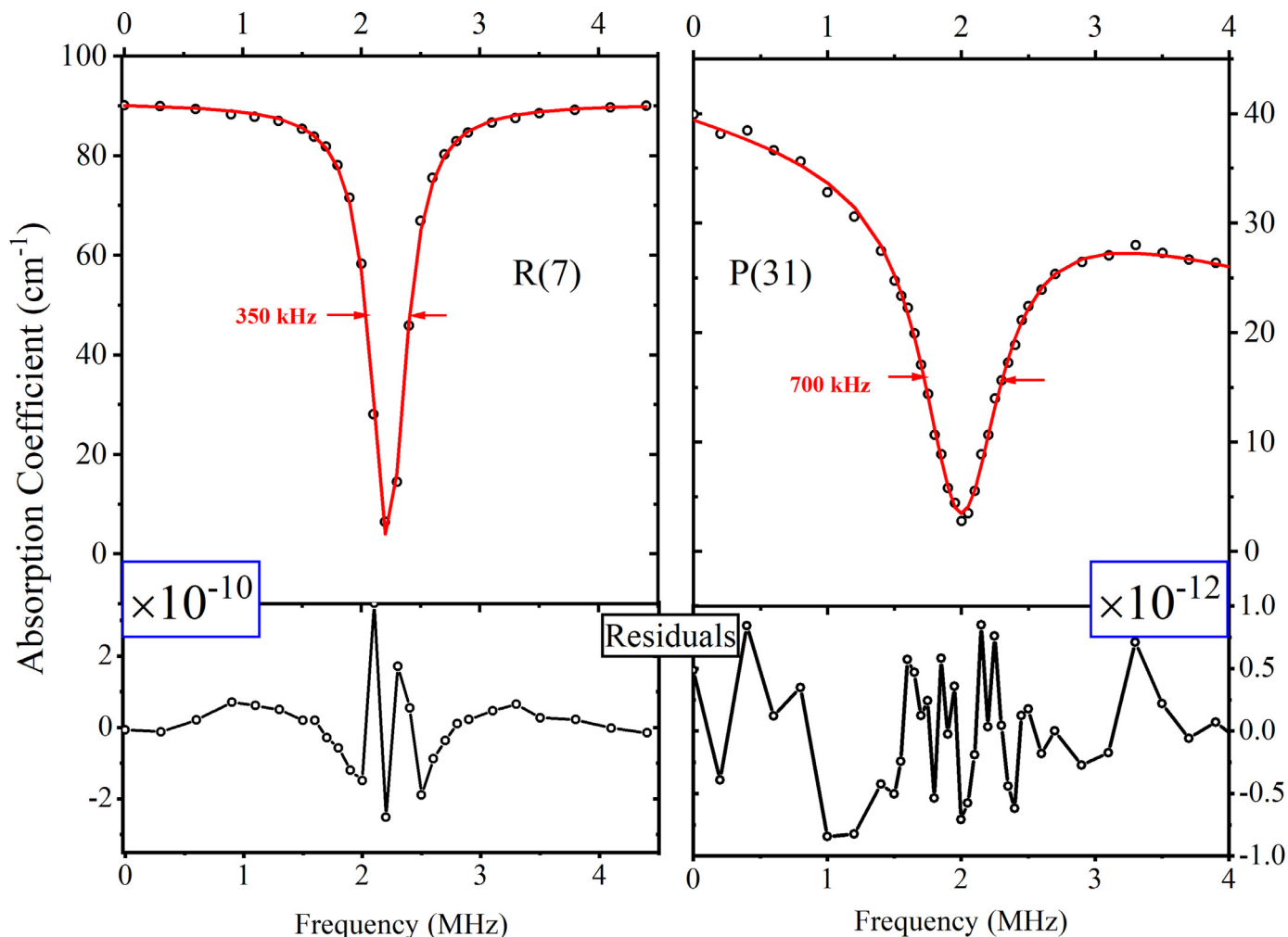
Fig. 1. Example of CRDS-saturation spectra for the R(7) (left panel) and P(31) (right panel) lines at the sample pressures of 0.3 Pa and 2.4 Pa, respectively, along with the residuals (lower panels) retrieved with a Lorentzian profile.

where $\nu_{R(J)}$ and $\nu_{P(J)}$ are the frequencies of the lines R(J) and P(J), respectively.

The fit resulted in four parameters with root mean squares (RMSs) of 4.5 and 2.7 kHz (b set) for the ground and second overtone vibrational states given in Table 2, together with the respective values in the literature [20,21,25]. The vibrational term G_v and another set (a) of the second overtone state's rotational parameters can be derived from a fit of 61 transition frequencies with the refined ground state constants determined in this work. The maximum J value used in the fit of the ground and upper levels are also given in Table 2. The (Exp.- Calc.) difference mostly ranges in the 1-σ experimental uncertainty region.

3.3. Comparison to literature

The line positions determined with the saturated spectrum in this work are believed to improve the accuracy for the line centers of $^{12}C^{16}O$ around 1.57 μm by two orders. Here, we make two alternative comparisons: (i) the line position comparison to the values provided in different line lists available in the literature; (ii) the ground state combination difference obtained from the P(J+1) and R(J-1) line positions comparison to those calculated with the sum of the R(J-1) and R(J+1) rotational frequencies from the microwave data.

3.3.1. Line position around 1.57 μm comparison

The line positions of $^{12}C^{16}O$ have been experimentally improved to the frequency accuracy of sub-MHz with comb-assisted cavity ring-down spectroscopy for 63 transitions around 1.57 um [25]. Recently, Cygan A. et al. in Torun used the cavity mode-width spectroscopy (CMWS) to determine the line positions of R(23) [26], R(24), and R(28) [27] with the 1-σ uncertainties of dozens kHz. Fig. 2 compares the experimental line positions from the comb-calibrated Doppler-broadened spectroscopy with our Lamb-dip measurements in the upper panel. The results are summarized as the frequency difference versus rotational quantum number m. All difference is within the 3-σ combined uncertainties. Note that the combined uncertainties mainly come from the Doppler-limited spectroscopy. In particular, the difference of CRDS-Grenoble's line list obeys normal distribution, confirming their line positions with the claimed accuracy of 300 kHz. While the difference is all found over 1-σ uncertainty for the values given by Torun's group. It seems that some errors might not be considered in their uncertainty analysis.

In Section 5 of Ref. [25], Mondelain D. et al. have made their line position values comparison to two various line lists derived with the mass-independent Dunham parameters: Farrenq et al.(1991) [28] and Velichko et al.(2012) [29], Coxon and Haji-georgiou's line list obtained with an empirical potential function [30], HITRAN2012 database [31], and Li et al. line list [32]. The
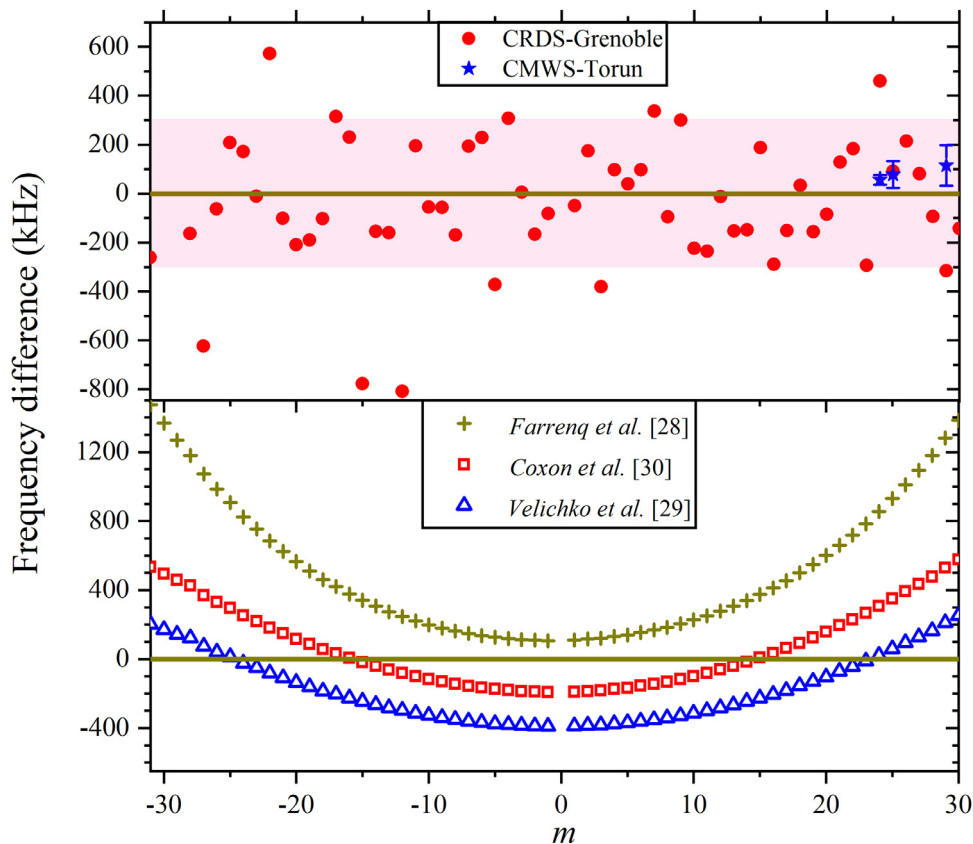
Fig. 2. Literature values difference (in kHz) from the saturated line positions versus the rotational quantum number m for 61 lines in the $3 \leftarrow 0$ band of $^{12}C^{16}O$. Error bars and pink shadow represent 1-σ combined uncertainties. Data sources are experimental values (upper panel) from CRDS-Grenoble (circle)[25], CMD(W)S-Torun (star)[26,27], and theoretical calculations (lower panel) from ref.[28] (cross), ref.[30] (open square), ref. [29] (open triangle).

comparison presented good agreements within 1 MHz for most line lists except Li's set. The experimental line positions from Refs. [25,27] were employed to HITRAN2016 [33] version in this region. So we only compare our values to Farreq's, Velichko's, Coxon's line list in the lower panel of Fig. 2. The calculated frequencies agree well with our measurements, with a difference within 400 kHz for most transitions. The difference increases with J'' and reaches 1.5 MHz for J''=31 transition of Farrenq's calculation. The mean deviations are 400.3 kHz, -169.1 kHz, and 75.6 kHz for Farrq's, Velichko's and Coxon's values, respectively. The calculated line positions with the mass-independent Dunham parameters has the smallest mean-square deviation 192.9 kHz by Velichko et al.'s derived with the critically evaluated input data using the Ritz principle.

3.3.2. Ground state combination difference comparison

The ground state combination difference ΔE can be calculated from the P(J+1) and R(J-1) line positions determined in this work, or from the R(J-1) and R(J+1) rotational frequencies in the rotational transitions with the following formula:

$$\Delta E(J) = \nu_{R_{3\leftarrow 0}(J-1)} - \nu_{P_{3\leftarrow 0}(J+1)} = \nu_{R_{0\leftarrow 0}(J+1)} + \nu_{R_{0\leftarrow 0}(J-1)} \cdots \quad (4)$$

The last column in Table 1 lists the ground state combination difference calculated with the Lamb-dip ro-vibrational frequencies in this work.

Varberg and Evenson from NIST [21] summarized the pure rotational line list ($\upsilon=0\leftarrow0$) with previous values (J''=0-4) by microwave spectrometer [34] and 26 measured values by tunable far-infrared spectroscopy (J''=5-37), gave the calculated rotational frequencies with the accuracy better than 5 kHz (1-σ) for $J''\leq28$. Lately, Winnewisser et al. improved the frequency accuracy to 0.5 kHz with the Lamb-dip measurements using the Cologne terahertz

spectrometer for J''=0-5 transitions. The Lamb-dip data together with the Doppler limited lines (J''=6-37) [35] resulted in four rotational spectroscopic parameters, which were used to calculate the CDMS [36] line list of $^{12}C^{16}O$. Another set of ground state combination difference can also be derived with the pure rotational frequencies.

Fig. 3 shows the ground state combination difference ΔE comparison derived from the pure rotational and the second overtone Lamb-dip frequencies. The difference of the nine pairs ground state combination difference (23 pairs in total) is outside the 1-σ combined uncertainty region (blue shaded), and deviates from the normal distribution by 8%. Most of the ground state combination difference ($J = 6 - 30$) from the Doppler-limited microwave spectroscopy in ref. [20] are larger than the values obtained from the saturated spectrum in this work. And it seems that there is a systematic deviation of about 1.3 kHz between our values and those in ref. [20] for J= 1 - 5, both calculated from the Lamb-dip frequencies.

The Lamb-dip spectrum of the R(2) and R(3) pure rotational transitions have been lately measured with the submillimeter-wave Lamb-dip spectrometer using a backward-wave oscillator radiation source referenced to a GPS disciplined rubidium clock by Golubiatnikov et al. [37], providing the Lamb-dip position uncertainties less than 1 kHz. These new data allow us to give one pair comparison with our value (red star). Note that the experimental uncertainty of R(3) is not available in ref. [37], set as 1 kHz in our comparison. Our ground state combination difference (J=3) agrees very well with Golubiatnikov's value with 0.1 kHz difference.

The single point comparison inspires us to find out two possible causes of the 1.3 kHz systematic deviation between our and CDMS's values: (i) The CDMS's values were obtained from the

Table 1
Positions of the lines in the second overtone band of $^{12}C^{16}O$ and the derived ground state combination difference (in kHz).

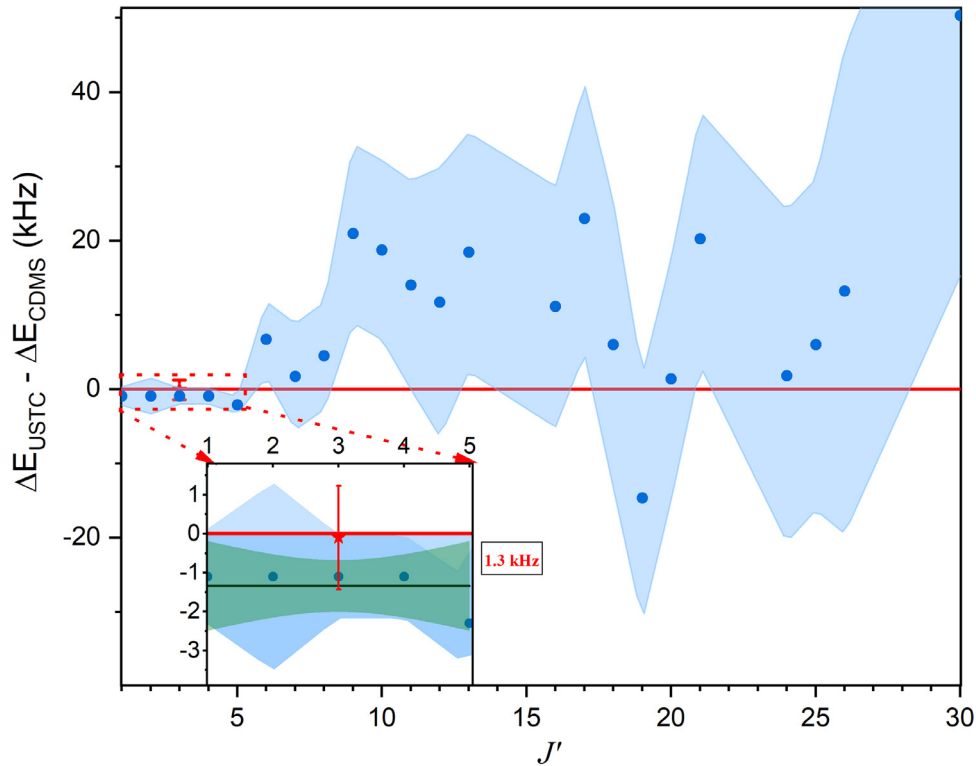| P(J")		R(J")		ΔE
P(1)	190266102171.1(07)			
P(2)	190147687256.1(06)	R(0)	190493496459.0(08)	345809202.6(10)
P(3)	190026133034.7(07)	R(1)	190602467025.7(22)	576333991.0(23)
P(4)	189901443912.0(06)	R(2)	190708280671.2(06)	806836759.2(08)
P(5)	189773624292.2(06)	R(3)	190810932992.0(06)	1037308699.8(08)
P(6)	189642678581.4(06)	R(4)	190910419590.5(07)	1267741009.1(09)
P(7)	189508611186.3(06)	R(5)	191006736062.1(06)	1498124875.8(08)
P(8)	189371426509.1(06)	R(6)	191099878013.6(06)	1728451504.5(08)
P(9)	189231128956.7(06)	R(7)	191189841045.4(08)	1958712088.7(10)
P(10)	189087722935.4(06)	R(8)	191276620759.7(06)	2188897824.3(08)
P(11)	188941212844.5(06)	R(9)	191360212764.0(05)	2418999919.5(08)
P(12)	188791603087.9(06)	R(10)	191440612665.1(05)	2649009577.2(08)
P(13)	188638898069.4(10)	R(11)	191517816071.9(06)	2878918002.5(15)
P(14)	188483102184.1(08)	R(12)	191591818592.9(06)	3108716408.8(10)
P(15)	188324219836.5(11)	R(13)	191662615838.4(06)	3338396001.9(13)
P(16)	188162255418.9(09)	R(14)	191730203422.8(07)	3567948003.9(11)
P(17)	187997213324.8(21)	R(15)	191794576958.9(09)	3797363634.1(23)
P(18)	187829097951.7(21)	R(16)	191855732061.0(08)	4026634109.3(22)
P(19)	187657913679.4(30)	R(17)	191913664346.6(09)	4255750667.2(31)
P(20)	187483664898.6(40)	R(18)	191968369435.4(08)	4484704536.8(41)
P(21)	187306355990.9(46)	R(19)	192019842945.7(41)	4713486953.8(62)
P(22)	187125991338.3(41)	R(20)	192068080491.3(41)	4942089153.8(58)
P(23)	186942575310.2(55)	R(21)	192113077706.3(41)	5170502396.1(69)
P(24)	186756112288.4(58)	R(22)	192154830203.8(43)	5398717915.4(72)
P(25)	186566606621.3(62)	R(23)	192193333610.7(43)	5626726989.4(75)
P(26)	186374062692(10)	R(24)	192228583548.3(54)	5854520856(12)
P(27)	186178484843(23)	R(25)	192260575646.0(65)	6082090803(24)
P(28)	185979877413(25)	R(26)	192289305529.4(87)	6309428116(26)
P(29)	185778244788(25)	R(27)	192314768824(20)	6536524036(32)
P(30)	185573591276(25)	R(28)	192336961145(20)	6763369869(32)
P(31)	185365921211(25)	R(29)	192355878133(20)	6989956922(32)

Fig. 3. Ground state combination difference ΔE (in kHz) obtained from the $P_{3 \leftarrow 0}(J + 1)$ and $R_{3 \leftarrow 0}(J - 1)$ line positions determined in this work compared to those calculated with the sum of the $R_{0 \leftarrow 0}(J - 1)$ and $R_{0 \leftarrow 0}(J + 1)$ rotational frequencies in the rotational transitions from ref.[20] (blue circle). The blue shadow covers the 1-σ combined uncertainty region. More details of energy difference comparison for $J=1 - 5$ are illustrated in the insert enlargement, together with the 68% confidence interval (green shadow) for the linear fit with the difference between this work and those in ref.[20].

Table 2

Spectroscopic constants (in kHz) of ground and the second overtone vibrational state.

Ground vibrational state				
Constant(kHz)	USTC (Hefei)		Cologne*JMS 184(1997): 468*	NIST*APJ 385(1992):763*
B_0 - 57635968	0.146(22)		0.019(28)	0.26(12)
D_0 -183	0.50653(14)		0.50489(16)	0.50552(46)
$H_0 \times 10^{-4}$	1.7412(33)		1.7168(10)	1.7249(59)
$L_0 \times 10^{-10}$	-10.5(24)		—	-3.1(23)
RMS	4.5		13	—
J_{max}	31		38	38
Second overtone vibrational state				
Constant	USTC (Hefei)			LIPhy (Grenoble)
(kHz)	a	b		
G_v	72.56(25)			43(72)
-190381373300				
B_v -56061900	10.1499(73)	10.153(23)		9.89(75)
D_v -183	0.477815(56)	0.47782(15)		0.4756(17)
$H \times 10^{-4}$	1.6079(14)	1.6079(38)		1.578(10)
$L_v \times 10^{-9}$	-1.07(11)	-1.05(28)		—
$Jmax$	30			33
RMS	3.1	2.7		263

The uncertainty (one standard deviation) in the last digits is in parentheses. RMS: root-mean-squares.
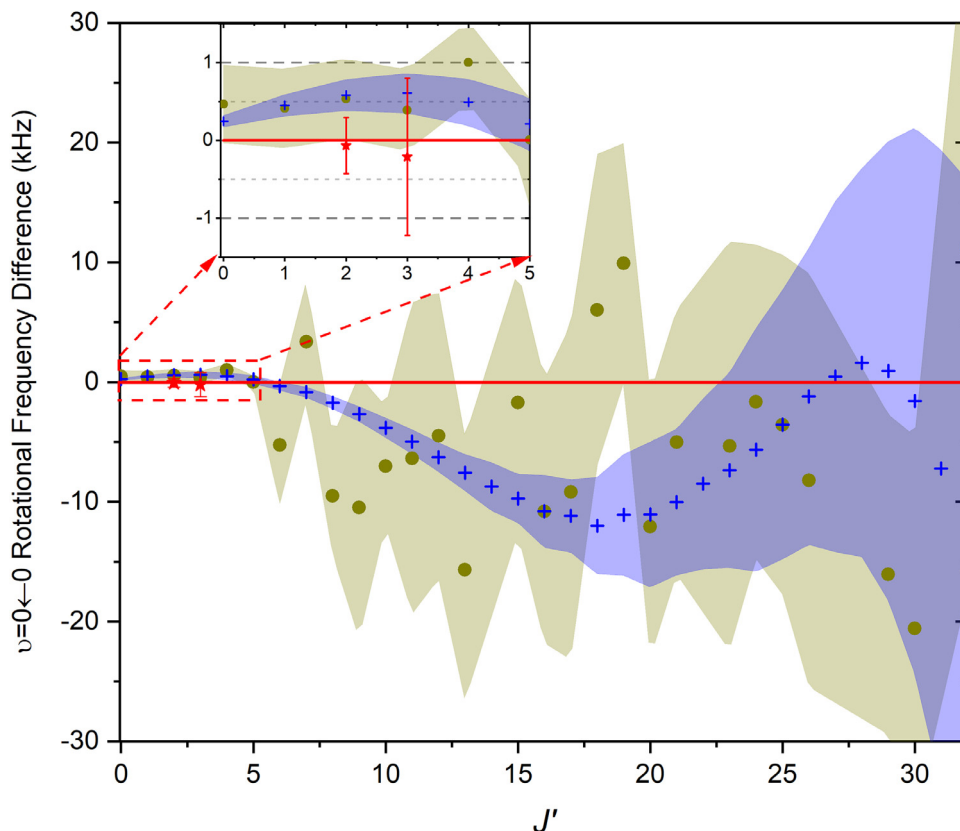
Fig. 4. $v = 0 \leftarrow 0$ rotational frequency difference (in kHz) between those calculated from the ground state spectroscopic parameters in this work and the experimental (circles) and calculated (crosses) line lists available in the literature [20] with relevant combined 1-σ uncertainties.

microwave spectrum measured without the GPS disciplined radio source. (ii) The ground state combination difference's systematic error is partly reduced with the subtraction of the ro-vibrational frequencies, while relatively increased with the addition of the pure rotational frequencies. Indeed, more rotational frequencies obtained with Golubiantnikov's similar spectrometer can lead to the real factors.

There is no doubt that our ground state combination difference ($J = 6 - 30$) has better accuracies. The new sets of the pure rotational frequencies ($v = 0 \leftarrow 0$, $v = 3 \leftarrow 3$) can be calculated with the ro-vibrational spectroscopic parameters derived in Table 2, at-tached as Supplementary Materials. Figs. 4 and 5 show the rotational frequency comparisons between the calculated values in this work and the line lists available in the literature [20,37,38] for the $v = 0 \leftarrow 0$ and $v = 3 \leftarrow 3$ bands, respectively. The calculated and experimental literature values of $J = 0 - 5$ transitions in the $v = 0 \leftarrow 0$ band agree within 1 kHz. Again, it seems that CDMS's values may have 0.5 kHz systematic deviation, equivalent to their 1-σ experimental error. The CDMS's values of $J = 6$-20 [20] definitely deviate from the real values with several kHz. There is a clear nonlinear difference of the calculated rotational frequencies in ref. [38] from our calculations in the $v = 3 \leftarrow 3$ band. In
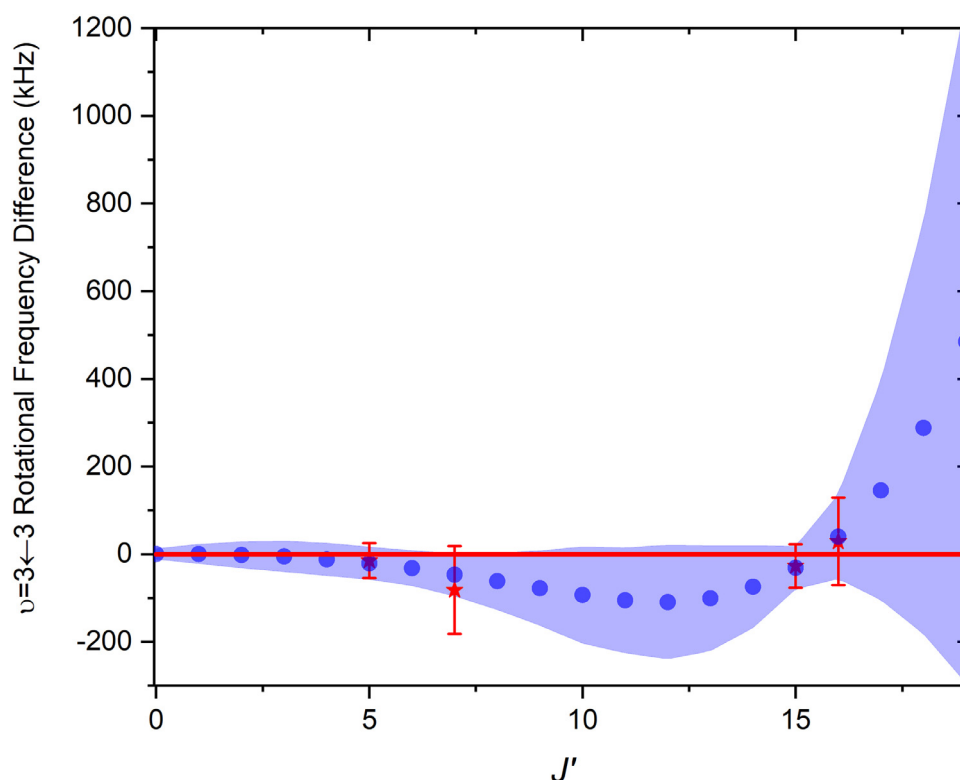
Fig. 5. $\upsilon = 3 \leftarrow 3$ rotational frequency difference (in kHz) between those calculated from $v=3$ vibrational state spectroscopic parameters in this work and the experimental values (stars), the calculated values (circles) in the literature [38] together with the combined 1-σ uncertainties.

general, most rotational frequencies' accuracy is improved on the magnitude of 1-2 orders.

4. Conclusions

Here we present the precisely Doppler-free absorption spectroscopy study of the P(31) – R(29) 61 lines in the second overtone band of $^{12}C^{16}O$ using a laser-locked cavity ring-down spectrometer referenced to an optical frequency comb. The line centers are determined with an accuracy of a few kHz for the lines with a wide intensity range of three orders of magnitude. The ground state's independent spectroscopic parameters are obtained with 30 ground state combination difference. It leads to a refinement of the ro-vibrational spectroscopic constants of the second overtone vibrational state with a RMS of 3.1 kHz. The pure rotational line lists of the $\upsilon = 0 \leftarrow 0$ and $\upsilon = 3 \leftarrow 3$ bands are constructed with sub-kHz accuracy to several kHz. Not only the high precision line positions around 1.57 μm may be used as frequency standards for the C-telecom band [39], but also the pure rotational frequencies with better accuracies will be beneficial for some astronomical studies observed by the Atacama Large Millimeter Array (ALMA) [4,40].

Declaration of Competing Interest

We declare that we have no conflict of interest.

Acknowledgement

Supplementary materials

Supplementary material associated with this article can be found, in the online version, at doi:10.1016/j.jqsrt.2021.107717.

References

[1] Krasnopolsky VA. Observations of the CO dayglow at 4.7 μm on Mars: variations of temperature and CO mixing ratio at 50km. Icarus 2014;228:189–96. doi:10.1016/j.icarus.2013.10.008.

[2] Madhusudhan N. Exoplanetary atmospheres: key insights, challenges, and prospects. Annu Rev Astron Astrophys 2019;57:617–63. doi:10.1146/annurev-astro-081817-051846.

[3] Lu N, Zhao Y, Díaz-Santos T, Xu CK, Gao Y, Armus L, et al. A Herschel space observatory spectral line survey of local luminous infrared galaxies from 194 to 671 microns. Astrophys J Suppl Ser 2017;230:1. doi:10.3847/1538-4365/aa6476.

[4] Vlemmings W, Khouri T, O'Gorman E, De Beck E, Humphreys E, Lankhaar B, et al. The shock-heated atmosphere of an asymptotic giant branch star resolved by ALMA. Nat Astron 2017;1:848–53. doi:10.1038/s41550-017-0288-9.

[5] Khouri T, Vlemmings WHT, Olofsson H, Ginski C, De Beck E, Maercker M, et al. High-resolution observations of gas and dust around Mira using ALMA and SPHERE/ZIMPOL. Astron Astrophys 2018;620. doi:10.1051/0004-6361/201833643.

[6] Mahadevan S, Ge J. The use of absorption cells as a wavelength reference for precision radial velocity measurements in the near-infrared. Astrophys J 2009;692:1590–6. doi:10.1088/0004-637X/692/2/1590.

[7] Benatti S. Multi-wavelength high-resolution spectroscopy for exoplanet detection: motivation, instrumentation and first results. Geosci 2018;8. doi:10.3390/geosciences8080289.

[8] Burkart J, Sala T, Romanini D, Marangoni M, Campargue A, Kassi S. Saturated CO_2 absorption near 1.6 μ m for kilohertz-accuracy transition frequencies. J Chem Phys 2015;142. doi:10.1063/1.4921557.

[9] Gatti D, Gotti R, Gambetta A, Belmonte M, Galzerano G, Laporta P, et al. Comb-locked Lamb-dip spectrometer. Sci Rep 2016;6:1–8. doi:10.1038/srep27183.

[10] Santamaria L, Di Sarno V, De Natale P, De Rosa M, Inguscio M, Mosca S, et al. Comb-assisted cavity ring-down spectroscopy of a buffer-gas-cooled molecular beam. Phys Chem Chem Phys 2016;18:16715–20. doi:10.1039/C6CP02163H.

[11] Truong GW, Long DA, Cygan A, Lisak D, Van Zee RD, Hodges JT. Comb-linked, cavity ring-down spectroscopy for measurements of molecular transition frequencies at the kHz-level. J Chem Phys 2013;138. doi:10.1063/1.4792372.

[12] Wang J, Sun YR, Tao LG, Liu AW, Hua TP, Meng F, et al. Comb-locked cavity ring-down saturation spectroscopy. Rev Sci Instrum 2017;88. doi:10.1063/1.4980037.

[13] Wang J, Sun YR, Tao LG, Liu AW, Hu SM. Communication: molecular near-infrared transitions determined with sub-kHz accuracy. J Chem Phys 2017;147. doi:10.1063/1.4998763.

[14] Chen J, Hua TP, Tao LG, Sun YR, Liu AW, Hu SM. Absolute frequencies of water lines near 790 nm with 10^{-11} accuracy. J Quant Spectrosc Radiat Transf 2018;205:91–5. doi:10.1016/j.jqsrt.2017.10.009.

[15] Kang P, Wang J, Liu GL, Sun YR, Zhou ZY, Liu AW, et al. Line intensities of the 30011e –00001e band of $^{12}C^{16}O_2$ by laser-locked cavity ring-down spectroscopy. J Quant Spectrosc Radiat Transf 2018;207:1–7. doi:10.1016/j.jqsrt.2017.12.013.

[16] Tao LG, Liu AW, Pachucki K, Komasa J, Sun YR, Wang J, et al. Toward a determination of the proton-electron mass ratio from the Lamb-dip measurement of hd. Phys Rev Lett 2018;120:1–5. doi:10.1103/PhysRevLett.120.153001.

[17] Tao LG, Hua TP, Sun YR, Wang J, Liu AW, Hu SM. Frequency metrology of the acetylene lines near 789 nm from Lamb-dip measurements. J Quant Spectrosc Radiat Transf 2018;210:111–15. doi:10.1016/j.jqsrt.2018.02.021.

[18] Wu H, Hu C Le, Wang J, Sun YR, Tan Y, Liu AW, et al. A well-isolated vibrational state of CO_2 verified by near-infrared saturated spectroscopy with kHz accuracy. Phys Chem Chem Phys 2020;22:2841–8. doi:10.1039/c9cp05121j.

[19] Ma LS, Ye J, Dubé P, Hall JL. Ultrasensitive frequency-modulation spectroscopy enhanced by a high-finesse optical cavity: theory and application to overtone transitions of C_2H_2 and C_2HD. J Opt Soc Am B 1999;16:2255. doi:10.1364/JOSAB.16.002255.

[20] Winnewisser G, Belov SP, Klaus T, Schieder R. Sub-Doppler measurements on the rotational transitions of carbon monoxide. J Mol Spectrosc 1997;184:468–72. doi:10.1006/jmsp.1997.7341.

[21] Varberg TD, Evenson KM. Accurate far-infrared rotational frequencies of carbon monoxide. Astrophys J 1992;385:763. doi:10.1086/170983.

[22] Madej AA, Alcock AJ, Czajkowski A, Bernard JE, Chepurov S. Accurate absolute reference frequencies from 1511 to 1545 nm of the $\nu_1+\nu_3$ band of $^{12}C_2H_2$ determined with laser frequency comb interval measurements. J Opt Soc Am B 2006;23:2200. doi:10.1364/JOSAB.23.002200.

[23] Edwards CS, Margolis HS, Barwood GP, Lea SN, Gill P, Rowley WRC. High-accuracy frequency atlas of $^{13}C_2H_2$ in the 1.5 μm region. Appl Phys B Lasers Opt 2005;80:977–83. doi:10.1007/s00340-005-1851-0.

[24] Madej AA, Bernard JE, John Alcock A, Czajkowski A, Chepurov S. Accurate absolute frequencies of the $\nu_1+\nu_3$ band of $^{13}C_2H_2$ determined using an infrared mode-locked Cr:YAG laser frequency comb. J Opt Soc Am B 2006;23:741. doi:10.1364/JOSAB.23.000741.

[25] Mondelain D, Sala T, Kassi S, Romanini D, Marangoni M. Broadband and highly sensitive comb-assisted cavity ring down spectroscopy of CO near 1.57 μm with sub-MHz frequency accuracy. J Quant Spectrosc Radiat Transf 2015;154:35–43. doi:10.1016/j.jqsrt.2014.11.021.

[26] Cygan A, Wcisło P, Wójtewicz S, Kowzan G, Zaborowski M, Charczun D, et al. High-accuracy and wide dynamic range frequency-based dispersion spectroscopy in an optical cavity. Opt Express 2019;27:21810. doi:10.1364/oe.27.021810.

[27] Cygan A, Wójtewicz S, Kowzan G, Zaborowski M, Wcisło P, Nawrocki J, et al. Absolute molecular transition frequencies measured by three cavity-enhanced spectroscopy techniques. J Chem Phys 2016;144. doi:10.1063/1.4952651.

[28] Farrenq R, Guelachvili G, Sauval AJ, Grevesse N, Farmer CB. Improved Dunham coefficients for CO from infrared solar lines of high rotational excitation. J Mol Spectrosc 1991;149:375–90. doi:10.1016/0022-2852(91)90293-J.

[29] Velichko TI, Mikhailenko SN, Tashkun SA. Global Multi-isotopologue fit of measured rotation and vibration–rotation line positions of CO in $X^1\Sigma^+$ state and new set of mass-independent Dunham coefficients. J Quant Spectrosc Radiat Transf 2012;113:1643–55. doi:10.1016/j.jqsrt.2012.04.014.

[30] Coxon JA, Hajigeorgiou PG. Direct potential fit analysis of the $X^1\Sigma^+$ ground state of CO. J Chem Phys 2004;121:2992–3008. doi:10.1063/1.1768167.

[31] Rothman LS, Gordon IE, Babikov Y, Barbe A, Chris Benner D, Bernath PF, et al. The HITRAN2012 molecular spectroscopic database. J Quant Spectrosc Radiat Transf 2013;130:4–50. doi:10.1016/j.jqsrt.2013.07.002.

[32] Li G, Gordon IE, Rothman LS, Tan Y, Hu SM, Kassi S, et al. Rovibrational line lists for nine isotopologues of the co molecule in the $X^1\Sigma^+$ ground electronic state. Astrophys J 2015;216 Suppl Ser. doi:10.1088/0067-0049/216/1/15.

[33] Gordon IE, Rothman LS, Hill C, Kochanov RV, Tan Y, Bernath PF, et al. The HITRAN2016 molecular spectroscopic database. J Quant Spectrosc Radiat Transf 2017;203:3–69. doi:10.1016/j.jqsrt.2017.06.038.

[34] Belov SP, Tret'iakov MI, Suenram RD. Improved laboratory rest frequency measurements and pressure shift and broadening parameters for the $J = 2 - 1$ and $J = 3 - 2$ rotational transitions of CO. Astrophys J 1992;393:848. doi:10.1086/171551.

[35] Belov SP, Lewen F, Klaus T, Winnewisser G. The rQ4 branch of HSSH at 1.25 THz. J Mol Spectrosc 1995;174:606–12. doi:10.1006/jmsp.1995.0029.

[36] Endres CP, Schlemmer S, Schilke P, Stutzki J, Müller HSP. The cologne database for molecular spectroscopy, CDMS, in the virtual atomic and molecular data centre, VAMDC. J Mol Spectrosc 2016;327:95–104. doi:10.1016/j.jms.2016.03.005.

[37] Golubiatnikov GY, Belov SP, Leonov II, Andriyanov AF, Zinchenko II, Lapinov AV, et al. Precision sub-Doppler millimeter and submillimeter Lamb-dip spectrometer. Radiophys Quantum Electron 2014;56:599–609. doi:10.1007/s11141-014-9464-2.

[38] Lewen F, Klapper G, Winnewisser G, Menten KM, Gendriesch R, Coxon JA, et al. Accurate laboratory rest frequencies of vibrationally excited CO up to v = 3 and up to 2 THz. Astron Astrophys 2009;497:927–30. doi:10.1051/0004-6361/200811539.

[39] Guelachvili G, Birk M, et al. High resolution wavenumber standards for the infrared. Pure Appl Chem 1996;68:193–208. doi:10.1351/pac199668010193.

[40] Pozzi F, Vallini L, Vignali C, Talia M, Gruppioni C, Mingozzi M, et al. CO excitation in the Seyfert galaxy NGC 7130. Mon Not R Astron Soc 2017;470:L64–8. doi:10.1093/mnrasl/slx077.